Effect of solvent on the microstructure and optical band gap of ZnO nanoparticles

Pravanjan Mallick*

Department of Physics, North Orissa University, Baripada 757 003, India

ZnO nanoparticles have been synthesized by chemical route using different solvents. X-ray diffraction characterization of the samples indicated ZnO nanoparticles crystallize in wurtzite phase with $\frac{c}{a}$ for all the samples is ~ 1.6. Though all the samples exhibit same crystal structure, the microstructure of ZnO nanoparticles is influenced with solvent. The ZnO nanoparticles have been synthesized using ethanol as solvent has smaller crystallite size than that obtained for ZnO nanoparticles synthesized using propanol and ethylene glycol as solvent. In accordance with crystallite size variation, the lowest and highest specific surface area has been calculated for ZnO nanoparticles synthesized using propanol and ethanol as solvent, respectively. Stress analysis using lattice parameter indicated that the crystallites of all ZnO samples experience compressive stress and the magnitude of the stress is nearly twice for ZnO nanoparticles synthesized with ethanol than that obtained for ZnO nanoparticles synthesized using ethylene glycol as solvent. UV-visible characterization of these samples indicated that the bang gap of ZnO nanoparticles is not affected much with the solvent. The refractive index and electron polarizability for all samples have been determined from the optical band gap of corresponding samples.

Keywords: ZnO nanoparticle, Microstructure, UV-visible

1 Introduction

In recent years, semiconductor nanoparticles have attracted much research attention due to their novel properties and wide spread technological application possibilities as compared to their bulk counterpart. ZnO is an important member of II-VI semiconductor with a direct band gap of 3.37 eV. ZnO shows large exciton binding energy (60 meV) which enables the device operation at low threshold voltage[1]. High localized exciton binding energy combined with unusual high exciton oscillator strength suggests the possibility of high field emission properties of ZnO even at room temperature[2]. ZnO has also been considered as a potential material for the use of the same in different applications such as solar cell[3], UV sensor[4], antimicrobial agent[5], photo detector[6], gas sensor[7], light emitting diode[8], optoelectronic[9], etc.

ZnO nanoparticles have been synthesized by various methods such as hydrothermal[10], precipitation[11], sol-gel[12], spray-pyrolysis[13], etc. Different synthesis methods have been shown to affect the microstructures like size, morphology, orientation, etc., which in turn influence the properties of the ZnO. Synthesis of ZnO nanoparticles with well controlled microstructure is of important for its use in various technological applications.

In the present work, ZnO nanoparticles have been synthesized by chemical route using different solvent with an aim to see the effect of solvent on the microstructure and optical band gap of ZnO nanoparticles.

2 Experimental

For the synthesis of ZnO nanoparticles in chemical route, zinc acetate ($Zn(CH_3COO)_2.2H_2O$) is used as starting material and ethanol, propanol and ethylene glycol are used as solvent. Zinc acetate (5 g) is dissolved in either of the solvent and the solution is stirred for half an hour. Then the solution is kept at 60 °C for 15 min. The resultant solution is kept for 1 day. Then the resultant product is dried at 200 °C. Finally the dried product is annealed at 550 °C to get the required ZnO nanoparticles used in the present study. ZnO nanoparticles were synthesized with ethanol, propanol and ethylene glycol hence forward named as ZnO-E, ZnO-P and ZnO-EG, respectively.

The structural and microstructural evolutions of ZnO nanoparticles were studied by X-ray diffraction with Cu K_α radiation using Bruker X-ray diffractometer (Model: D8 Advance). The optical

*E-mail: pravanjan_phy@yahoo.co.in

absorption spectroscopy of ZnO nanoparticles were performed using diffuse reflectance spectroscopy by a double beam UV-Visible spectrophotometer (Simadzu, UV-2450) with an integrating sphere assembly.

3 Results and Discussion

Figure 1 shows the XRD pattern of ZnO-E, ZnO-P and ZnO-EG synthesized by chemical route. All the peaks present in the XRD pattern indexed to the wurtzite phase (space group $P6_3mc$) of ZnO. In an earlier study on synthesis of CuO nanoparticle by chemical route using ethanol and propanol as solvent, it was seen that the microstructure of CuO nanoparticles influenced with solvent even though the structure remains same[14]. Interestingly by changing the solvent to ethylene glycol led to the synthesis of Cu$_2$O/CuO nanocomposite[15]. In the present case though the structure of ZnO nanoparticles synthesized with different solvent remains same but microstructure of ZnO might be influenced with the solvent. We therefore determine lattice parameter, crystallite size, bond length in the followings.

Lattice parameters, a along (100) plane and c along (002) plane of the ZnO nanoparticles synthesized with different solvents are determined using the following equation:

$$a = \frac{1}{\sqrt{3}} \frac{\lambda}{\sin\theta} \qquad \ldots (1)$$

and

$$c = \frac{\lambda}{\sin\theta} \qquad \ldots (2)$$

The ratio of $\frac{c}{a}$ for all the samples is ~ 1.6 which matches nicely with the hexagonal closed pack structure. We also determine the unit cell volume (V) and atomic packing fraction (APF) for all the ZnO samples using the following relation:

$$V = \frac{\sqrt{3}}{2} a^2 c \qquad \ldots (3)$$

and

$$APF = \frac{2\pi}{3\sqrt{3}} \left(\frac{a}{c} \right) \qquad \ldots (4)$$

The values of a, c, $\frac{c}{a}$, V and APF determined for ZnO-E, ZnO-P and ZnO-EG are presented in Table 1.

In order to see the effect of solvents on the microstructural properties of ZnO particles, we calculated the particle size and microstrain values using the relation[16]:

$$\frac{\beta\cos\theta}{\lambda} = \frac{1}{D} + \varepsilon\left(\frac{2\sin\theta}{\lambda} \right) \qquad \ldots (5)$$

where, $\beta, \lambda, \varepsilon, \theta$ and D are the FWHM (in radian), wavelength of Cuk_α radiation, microstrain, Bragg angle and average diameter of the ZnO particles, respectively. The Williamson–Hall (W-H) plot[16] (Fig. 2) of $\frac{\beta\cos\theta}{\lambda}$ vs. $\frac{2\sin\theta}{\lambda}$ gives the value of microstrain from the slope and crystallite size (diameter of the ZnO particles) from the ordinate
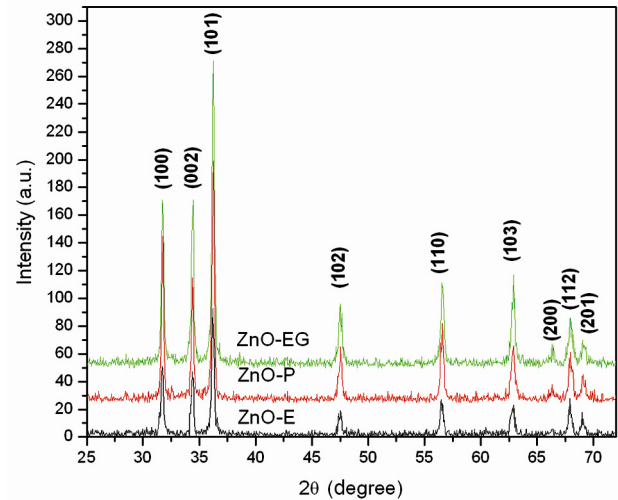

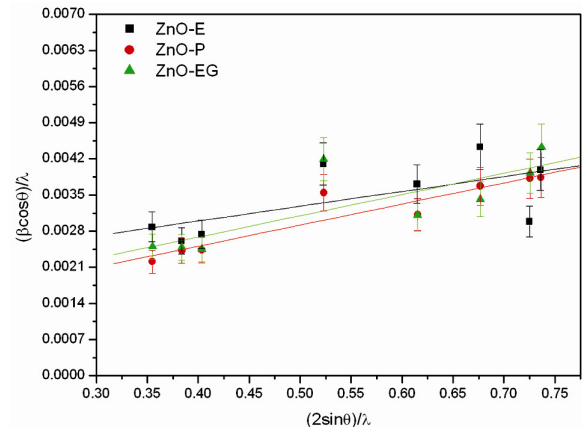Fig. 1 – XRD pattern of ZnO-E, ZnO-P and ZnO-EG synthesized by chemical route

Fig. 2 – Williamson–Hall (W-H) plot of $\frac{\beta\cos\theta}{\lambda}$ vs. $\frac{2\sin\theta}{\lambda}$ for ZnO-E, ZnO-P and ZnO-EG nanoparticles

Table 1 – The values of a, c, $\frac{c}{a}$, V, APF D and ε determined for ZnO-E, ZnO-P and ZnO-EG

Sample	a (Å)	c (Å)	$\frac{c}{a}$	V (Å³)	APF	D (nm)	ε (%)
ZnO-E	3.256	5.213	1.601	47.862	0.7551	54±4	0.287
ZnO-P	3.253	5.211	1.602	47.755	0.7546	115±8	0.409
ZnO-EG	3.253	5.210	1.6015	47.746	0.7548	96±7	0.412

intersection. The obtained values of crystallite size and microstrain for different ZnO samples are presented in (Table 1). The value of D is higher for ZnO-P and lower for ZnO-E.

The internal stress ($\frac{c}{a}$) is related to positional parameter[17] (u) and Zn-O bond length[18] (l) as per the following relations:

$$u = \frac{a^2}{3c^2} + 0.25 \qquad \ldots (6)$$

and
$$l = \sqrt{\frac{a^2}{3} + (0.5-u)^2 c^2} \qquad \ldots (7)$$

These values calculated for different ZnO samples are also given in Table 2. Zn-O bond length for all the samples in our case is ~ 1.98 matches well with the reported values[19-21]. One can determine the specific surface area (S_a) of the ZnO nanoparticles using the following relation[22]:

$$S_a = \frac{6}{\rho_s \times D} \qquad \ldots (8a)$$

where , ρ_s is the X-ray density which can be calculated as:

$$\rho_s = \frac{ZM}{N_A V} \qquad \ldots (8b)$$

Z is the number of formula units in the unit cell which is 2 for ZnO, M is molecular weight of the substance, N_A is Avogadro's number and V is the unit cell volume. The calculated value of ρ_s and S_a for ZnO-E, ZnO-P and ZnO-EG are given in Table 2. The particles with lowest S_a and the highest S_a are calculated for ZnO-P and ZnO-E, respectively. This observation is in accordance with the crystallite size variation (Table 1) as the smaller size particles show larger surface area.

Table 2 – The values of u, l, ρ_s and S_a determined for ZnO-E, ZnO-P and ZnO-EG

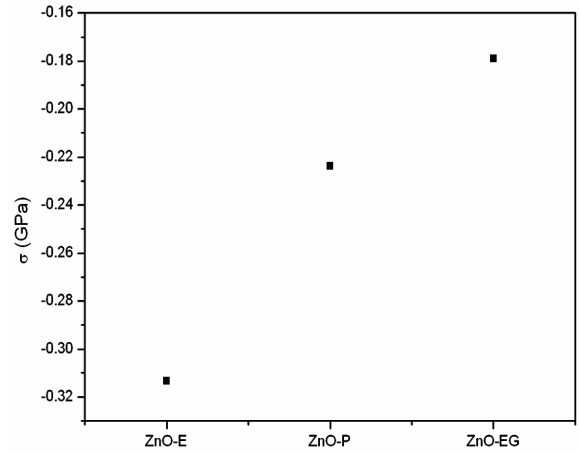| Sample	u	l (Å)	ρ_s (g/cm³)	S_a (cm²/g)×10⁵
ZnO-E	0.38005	1.98113	5.64845	1.96711
ZnO-P	0.37988	1.97968	5.66111	0.92162
ZnO-EG	0.37996	1.97951	5.66217	1.10382

Fig. 3 – Evolution of stress in ZnO-E, ZnO-P and ZnO-EG nanoparticles

The average uniform stress (σ) along c-axis in randomly oriented ZnO nanoparticles can be determined using the following expression[23]:

$$\sigma(GPa) = -233\left(\frac{c-c_{bulk}}{c_{bulk}}\right) \qquad \ldots (9)$$

where , c_{bulk} is the strain free lattice parameter of ZnO powder (5.206 Å). The negative sign in the calculated stress for all ZnO samples indicate that the crystallites experience compressive stress. The magnitude of the stress is nearly twice for ZnO-E than that of ZnO-EG (Fig 3).

Figure 4 shows the room temperature UV-Visible absorption spectra of ZnO nanoparticles synthesized with different solvents. The optical absorption coefficient (α) and optical band gap (E_g) are related by the following expression[24]:

$$\alpha = \frac{B(h\nu - E_g)^{n'}}{h\nu} \qquad ... (10)$$

where $h\nu$ is the incident photon energy and B is a materials dependent constant. The value of n' is ½ for direct inter-band transitions and/or 2 for indirect inter-band transitions. The linear relation observed for $(ah\nu)^2$ vs. $h\nu$ plot (Fig. 5) suggests that the ZnO nanostructures are direct band gap semiconductors. By extrapolating the linear portion of the $(ah\nu)^2$ versus $h\nu$ plot to $\alpha = 0$, we can estimate the optical band gap for ZnO-E (Fig. 5(a)), ZnO-P (Fig. 5(b)) and ZnO-EG (Fig. 5(c)) samples. The obtained values are presented in Table 2. All the samples seem to have better conductivity as they show lower band gap than the bulk ZnO which is ~ 3.37 eV. Similar type of observation, i.e., the observation of lower band gap than the bulk ZnO has been seen by Foo et al.[9] for ZnO thin films. ZnO with band gap ~3.2-3.4 eV is ideal for optical device applications like light-emitting diodes (LEDs), laser diodes, and photodetectors in the ultraviolet (UV) wavelength range[25]. Therefore ZnO nanoparticles synthesized in present case could be useful for various optical devices.

The absorption coefficient at lower photon energy usually follows the Urbach rule[26]:

$$\alpha(h\nu) = \alpha_0 \exp\left(\frac{h\nu}{E_u}\right) \qquad ... (11)$$

where, a_o is the constant and E_U is the Urbach energy. One can estimate the value of E_U from reciprocal of the slope of the linear portion of the $\ln\alpha$ versus $h\nu$ plot (Fig. 6). It has been reported that both static structural and dynamic phonon disorder[27] can be quantified through E_u. It has also been reported that for high quality crystalline semiconductors, E_u is a direct measure of temperature-induced disorder and for amorphous or highly doped materials, E_u becomes larger because of the contributions from both thermal and structural disorders[28]. The lowest and highest Urbach energy are calculated for ZnO-P and ZnO-EG (Table 3). This indicated that ZnO-EG samples has more structural disorder than, ZnO-E than ZnO-P.

Evaluation of refractive index (n) of the material is important as it is one of the important property for evaluation of potentiality of the materials for the use of them in integrated optical devices. Several models are there to calculate n using E_G of the material. Recently, Kumar and Singh[29] have proposed a model based on the experimental data to calculate the value
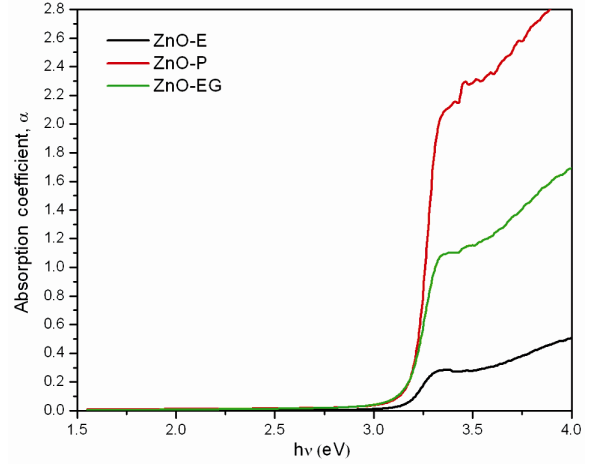

Fig. 4 – Room temperature UV-Visible absorption spectra of ZnO-E, ZnO-P and ZnO-EG nanoparticles
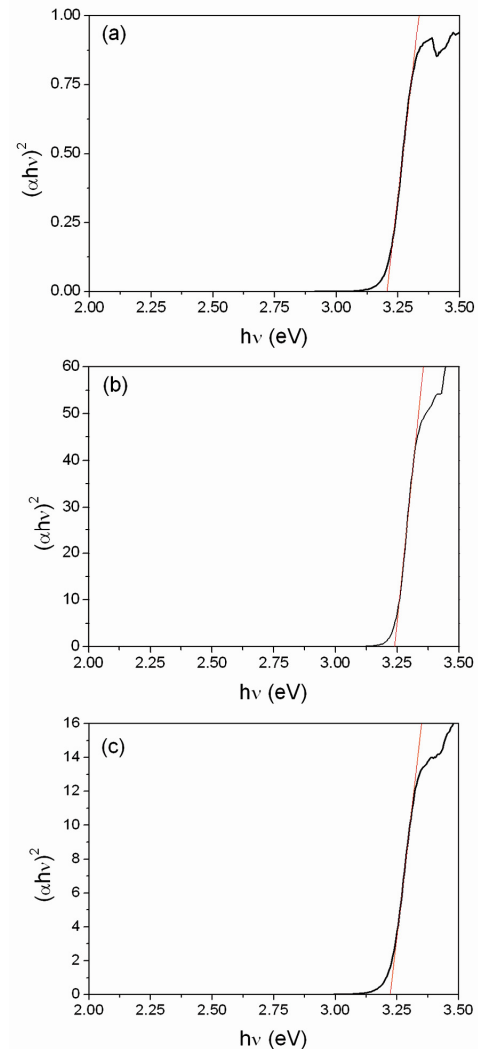

Fig. 5 – Variation of $(\alpha h\nu)^2$ vs. photon energy ($h\nu$) for (a) ZnO-E, (b) ZnO-P and (c) ZnO-EG nanoparticles
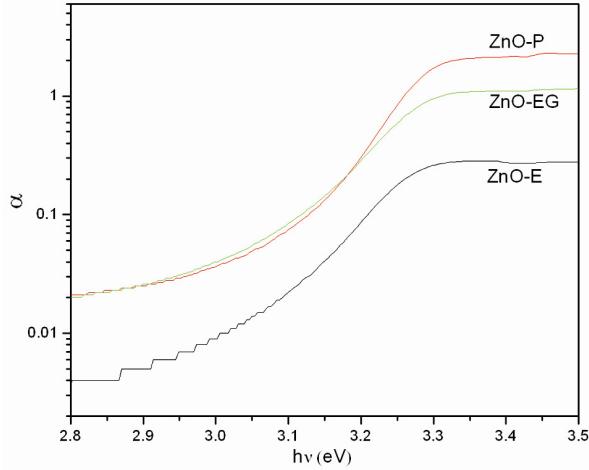
Fig. 6 – Variation of $\ln \alpha$ vs. $h\nu$ for ZnO-E, ZnO-P and ZnO-EG nanoparticles

Table 3 – The values of E_u, E_g, n, $\alpha'_{classical}$ and α' for ZnO-E, ZnO-P and ZnO-EG

Sample	E_u (eV)	E_g (eV)	n	$\alpha'_{classical}$ ($\times 10^{-24}$cm^3)	α' ($\times 10^{-24}$ cm^3)
ZnO-E	0.157	3.21	2.3117	3.3929	3.3971
ZnO-P	0.128	3.23	2.3059	3.3844	3.3868
ZnO-EG	0.168	3.22	2.3097	3.3899	3.3935

of n for mixed materials belonging to groups IV, II-VI, III-V semiconductors, insulators, oxides and halides. According this model, the relation between and E_g is given by:

$$n = KE_g^C \qquad \ldots (12)$$

where , $K = 3.3668$ and $C = -0.32234$. The 'n' is related to the electron polarizability (α') of ions and local field inside the material. One can use the classical theory to calculate $\alpha'_{classical}$ from for n and α' from E_g using the following relations [30, 31]:

$$\alpha'_{classical} = \frac{(n^2 - 1)}{(n^2 + 2)} \frac{M}{\rho} \times 0.395 \times 10^{-24}\, cm^3 \qquad \ldots (13)$$

and

$$\alpha' = \left[\frac{12.41 - 3\sqrt{E_g - 0.365}}{12.41} \right] \frac{M}{\rho} \times 0.395 \times 10^{-24}\, cm^3 \quad \ldots (14)$$

where M and ρ are molecular weight (g/mol) and density (g/cm^3) of the substances, respectively. The values of E_g, n, $\alpha'_{classical}$ and α' determined for ZnO nanoparticles synthesized with different solvent are presented in Table 3. The refractive index obtained in the present study matches well with the refractive index of ZnO nanoparticles[32].

4 Conclusions

We report the synthesis of ZnO nanoparticles by chemical route using three different solvents (ethanol, propanol and ethylene glycol). The structural characterization indicated ZnO nanoparticles crystallize in wurtzite phase. ZnO nanoparticles synthesized with ethanol show smaller crystallite size than that obtained for ZnO nanoparticles synthesized by propanol and ethylene glycol. Stress analysis using lattice parameter indicated that the crystallites of all ZnO samples experience compressive stress and the magnitude of the stress is nearly twice for ZnO nanoparticles synthesized with ethanol than that obtained for ZnO nanoparticles synthesized using ethylene glycol as solvent. UV-visible characterization of the samples indicated that the band gap and hence the refractive index and electron polarizability of ZnO nanoparticles are not affected much with the solvent. Our study indicated that ZnO nanoparticles could be useful for various optical devices.

References
1   Xing Y J, Xi Z H, Xue Z Q, Zhang X D, Song J H, Wang R M, Xu J, Song Y, Zhang S L & Yu D P, *Appl Phys Lett*, 83 (2003) 1689.
2   Sun Z, Zhao B & Lombardi J R, *Appl Phys Lett*, 91 (2007) 221106.
3   Guillen E, Azaceta E, Peter L M, Zukal A, Tena-Zaera R & Anta J A, *Energy Environ Sci*, 4(9) (2011) 3400.
4   Bai S, Wu W, Qin Y, Cui N, Bayerl D J & Wang X, *Adv Funct Mater*, 21 (2011) 4464.
5   Zhang L, Ding Y, Povey M & York D, *Prog Nat Sci*, 18 (2008) 939.
6   Liewhiran C & Phanichphant S, *Sensors*, 7 (2007) 1159.
7   Barreca D, Bekermann D, Comini E, Devi A, Fischer R A, Gasparotto A, Maccato C, Sberveglieri G & Tondello E, *Sensor Actuat-B Chem*, 149(1) (2010) 1.
8   Tsukazaki A, Ohtomo A, Onuma T, Ohtani M, Makino T, Sumiya M, Ohtani K, Chichibu S F, Fuke S, Segawa Y, Ohno H, Koinuma H & Kawasaki M, *Nature Mater*, 4 (2005) 42.

9   Foo K L, Kashif M, Hashim U & Liu W-W, *Ceram Int*, 40 (2014) 753.

10   Ismail A A, El-Midany A, Abdel-Aal E A & El-Shall H, *Mater Lett*, 59(14) (2005) 1924.

11   Rath C, Mallick P, Pandey D, Sa D, Banerjee A & Mishra N C, *J Phys Condens Matter*, 21 (2009) 075801.

12   Golić D L, Branković G, Nešić M P, Vojisavljević K, Rečnik A, Daneu N, Bernik S, Šćepanović M, Poleti D & Branković Z, *Nanotechnology*, 22 (2011) 395603.

13   Lee S D, Nam S H, Kim M H & Boo J H, *Phys Procedia*, 32 (2012) 320.

14   Mallick P & Sahu S, *Nanosci Nanotechnol*, 2(3) (2012) 71.

15   Mallick P, *Proc Nat Acad Sci Sec A*, 84 (2014) 387.

16   Williamson G K & Hall W H, *Acta Metall*, 1 (1953) 22.

17   Özgür Ü, Alivov Ya I, Liu C, Teke A, Reshchikov M A, Doğan S, Avrutin V, Cho S-J & Morkoç H, *J Appl Phys*, 98 (2005) 041301.

18   Mote V D, Purushotham Y & Dole B N, *Cryst Res Technol*, 46 (2011) 705.

19   Chen L, Xiong Z, Wan Q & Li D, *Opt Mater*, 32 (2010) 1216.

20   Proffit D E, Ma Q, Buchholz D B, Chang R P H, Bedzyk M J & Mason T O, *J Am Ceram Soc*, 95 (2012) 3657.

21   Zhang L, Li J, Du Y, Wang J, Wei X, Zhou J, Cheng J, Chu W, Jiang Z, Huang Y, Yan C, Zhang S & Wu Z, *New J Phys*, 14 (2012) 013033.

22   Tripathi A K, Singh M K, Mathpal M C, Mishra S K & Agarwal A, *J Alloys Compounds*, 549 (2013) 114.

23   Lupan O, Pauporte T, Chow L, Viana B, Pelle F, Ono L K, Cuenya B R & Heinrich H, *Appl Surf Sci*, 256 (2010) 1895.

24   Mott N F & Davies E A, *Electronic processes in non-crystalline materials*, (Clarendon Press, Oxford,) 1979.

25   Sawyer S, Qin L & Shing C, *Int J High Speed Electron Syst*, 20 (2011) 183.

26   Urbach F, *Phys Rev*, 92 (1953) 1324.

27   Cody G D, Tiedje T, Abales B & Goldstein Y, *Phys Rev Lett*, 47 (1981) 1480.

28   Abay B, Guder H S, Efeoglu H & Yogurtcu Y K, *J Phys Chem Solids*, 62 (2001) 747.

29   Kumar V & Singh J K, *Indian J Pure Appl Phys*, 48 (2010) 571.

30   Ahmad S, Ashraf M, Ahmad A & Singh D V, *Arab J Sci Eng*, 38 (2013) 1889.

31   Mallick P, Mishra D K, Kumar P & Kanjilal D, *Mater Sci Poland*, 33 (2015) 555.

32   Ismail R A, Habubi N F & Abid H R, *Int Lett Chem Phys Astro*, 23 (2014) 37.